Energy Conversion and Management 73 (2013) 106–120

Contents lists available at SciVerse ScienceDirect

Energy Conversion and Management

journal homepage: www.elsevier.com/locate/enconman

Energetic and exergetic analyses of T56 turboprop engine

Ozgur Balli [a,*], Arif Hepbasli [b]

[a] First Air Supply and Maintenance Center, TurAF, Eskisehir, Turkey
[b] Depertment of Energy Systems Engineering, Faculty of Engineering, Yasar University, 35100 Bornova, Izmir, Turkey

ARTICLE INFO

Article history:
Received 9 December 2012
Accepted 10 April 2013
Available online 17 May 2013

Keywords:
Energy analysis
Exergy analysis
Energetic efficiency
Exergetic efficiency
Improvement potential
Fuel-production ratio

ABSTRACT

This study presents the results of energetic and exergetic analyses of T56 turboprop engine at various power loading operation modes (75%, 100%, Military and Takeoff). The energetic and exergetic performance evaluations were made for both the shaft power (Case A) and the shaft power plus the kinetic energy of exhaust gaseous (Case B). The energetic efficiency was calculated to be maximum at 25.4% for Case A and 28.1% for Case B while the exergy efficiency was obtained to be maximum at 23.8% for Case A and 26.3% for Case B at Takeoff mode, respectively. The maximum exergy destruction rate occurred within the combustion chamber. It increased from 4846.3 kW to 6234.1 kW depending on operation modes. The exergetic performance parameters, such as the relative exergy consumption, the fuel depletion ratio, the productivity lack ratio, the improvement potential and the fuel-production ratio, were also investigated. The fuel energy-production ratio decreased from 4.6 to 3.9 while the fuel exergy-production ratio decreased from 4.9 to 4.2 by increasing the produced shaft power and residual thrust. The results provided here can be helpful to regulate and select operation modes for these engine users.

1. Introduction

The future world economy is envisioned to be truly global where national boundaries become diffused by interdependent commerce. This future vision only can be realized if there is a revolutionary change in transportation systems, enabling greater mobility of people and products with improved safety, timeliness and convenience. Propulsion and power capabilities are the foundation, on which future subsonic and supersonic transport aircraft will shape the aviation landscape and establish this global conduit of commerce. Propulsion innovations have been the fundamental driver for progress in air transportation. Enormous advances in propulsion performance and efficiency have made it possible for aircraft to travel at higher speeds over longer distances while carrying larger payloads [1]. Over the period 1989–2009, total scheduled traffic, measured in tone kilometers performed, grew at an average annual rate of 4.4%. In 2009, the world's airlines carried about 2.3 billion passengers and 38 million tons of freight on scheduled services [2]. Aviation energy consumption and emissions are expected to increase and constitute a greater proportion of the total anthropogenic climate impact. Air transport growth has outpaced reductions in energy intensity and will continue to do so through the foreseeable future, perhaps by an increased margin. Unless measures are taken to significantly alter the dominant historical rates of change in technology and operations, the impact of aviation emissions on local air quality and climate will continue to grow [3]. Given the world's finite natural resources and growing energy demands, it is increasingly important to understand energy and resources degradation and to improve systems while reducing environmental impact [4].

The environmental impact of emissions can be reduced by increasing the efficiency of fuel utilization [5]. Thermodynamic analysis (energy and exergy) has been used to assess the efficiency and the performance of all thermal systems. Energy analysis deals with the quantity of energy. It merely serves as a necessary tool for keeping of energy during a process. However, the exergy analysis considers the quality of energy. Exergy is related to the degradation of energy during a process, the entropy generation, and the lost opportunities to do work. It is well-known that exergy can be used as a potential tool to determine the location, type and true magnitude of exergy losses and destructions [6]. In the open literature, several studies have been reported to evaluate the energetic, exergetic, exergeconomic and exergoenvironmental performances of aircraft engines. The effect of the reference environment at different altitudes on the aircraft engine performance was investigated. Etele and Rosen [7] performed an exergy analysis to examine the effects of using difference reference-environment models on a turbojet engine over flight attitudes ranging from sea level to 15,000 m. The actual rational efficiency of turbojet decreased with increasing altitude, ranging from a value of 16.9% at sea level to 15.3% at 15,000 m. Turgut et al. [8] made an exergy analysis of a turbofan kerosene-fired engine with augmenter at sea level and an altitude of 11,000 m. Exergy destructions and exergy

* Corresponding author. Tel.: +90 5366771826.
E-mail address: balli07balli@yahoo.com (O. Balli).

0196-8904/$ - see front matter © 2013 Elsevier Ltd. All rights reserved.
http://dx.doi.org/10.1016/j.enconman.2013.04.014

Nomenclature

A	area (m^2)
c_P	specific heat capacity (kJ/kg K)
$\dot{E}$	energy rate (kW)
$\dot{E}x$	exergy rate (kW)
$\dot{E}IP$	energetic improvement potential (kW)
ESP	equivalent shaft power (kW)
$\dot{E}xIP$	exergetic improvement potential (kW)
F	thrust (kN)
FPR	fuel-production ratio
LHV	lower heating value of fuel (kJ/kg)
$\dot{m}$	mass flow rate (kg/s)
P	pressure (kPa)
$\dot{Q}$	heat transfer rate (kW)
SFC	specific fuel consumption (kg/kW h)
T	temperature (K)
V	velocity (m/s)
$\dot{W}$	work rate or power rate(kW)

Greek letters

α	fuel exergy depletion ratio (%)
β	productivity lack ratio in exergetic term (%)
χ	relative exergy consumption ratio (%)
ε	specific exergy (kJ/kg)
ϕ	fuel energy depletion ratio (%)
φ	productivity lack ratio in energetic term (%)
λ	specific heat capacity equation constant
γ	fuel exergy grade function
η	energetic efficiency (%)
μ	specific heat ratio
θ	relative energy losses ratio (%)
ξ	combustion reaction equation constant
ψ	exergetic efficiency (%)

Subscripts

a	air
AC	air compressor
Acc	accessory
C	consumption (destruction and losses)
CC	combustion chamber
ch	chemical
D	destruction
ED	exhaust duct
en	energy
ex	exergy
f	fuel
g	combustion gas
GT	gas turbine
$GTMS$	gas turbine mechanical shaft
in	input
j	the j'th component
k	location
kn	kinetic
L	losses
out	output
ph	physical
Pr	product
pt	potential
RGB	reduction gearbox
T	temperature
TPE	turboprop engine
0	dead (environment or reference) state

efficiency of each component of the engine were determined. The augmenter unit had the highest exergy destruction with 48.1% of the whole engine at the sea level, followed by the exhaust, the combustion chamber and the turbine, amounting 29.7%, 17.2% and 2.5%, respectively. Turan [9] also analyzed the effect of the reference altitudes on the exergetic efficiency of a turbofan engine with the aid of specific exergy method. The exergetic efficiency of the engine was calculated to be 50.3% at 4000 m to 48.9% at 9000 m. These studies indicated that an increase in the reference altitude decreased the exergetic efficiency and increased the energetic efficiency of the engine.

Exergoeconomics or thermoeconomic is the branch of engineering that appropriately combines, at the level of system components, thermodynamic evaluations based on an exergy analysis with economic principles, in order to provide the designer or operator of a system with information that is useful to the design and operation of a cost-effective system [10]. Balli et al. [11] studied the exergy and exergoeconomic analyses of an aircraft jet engine as named J69-T25A used on T-37B/C model training aircraft. The exergetic efficiency of the engine was accounted to be 34.8% for 2421.9 kW-exhaust gases product. The exergy cost and unit exergy cost of the jet engine exhaust gases were 618.6 $/h and 70.96 $/GW, respectively. Turgut et al. [12] developed the thrust cost rate parameter for turbofan engine. The thrust cost rate was accounted to be 138.9 $/h/kN for fan thrust and 304.4 $/h/kN for core engine thrust, respectively. Aydin et al. [13] investigated the exergetic and exergoeconomic analyses of a turboprop engine with a free power turbine used for medium-range twin-engine transport plane that was jointly developed as a regional airliner and military transport. The exergy cost and the unit exergy cost of the shaft power were determined to be 396 $/h and 78.5 $/GW, respectively

Exergoenvironmental analysis was developed to investigate the formation of environmental impacts associated with energy conversion systems at component level, and to generate information crucial for designing systems with a lower overall environmental impact. In the exergoenvironmental analysis, Life Cycle Assessment is appropriately combined with the exergy analysis. This combination is based on the methodological approach of the exergoeconomic analysis. Environmental impacts are assigned to the exergy streams of the system. The method generates information on impacts associated with the thermodynamic inefficiencies (exergy destruction) on the one hand, and on impacts associated with the construction, operation, maintenance and disposal of components on the other [14]. The exergoenvironmental analysis can be used to monitor the environmental impacts of aircraft engine on the flight envelops. Altuntas et al. [15] performed the exergoenvironmental performance of a four cylinder, spark ignition, naturally aspirated and air-cooled piston-prop aircraft engine for landing takeoff and cruise phases. The maximum specific environmental impact of the production was estimated to be 12.2 mPts/MJ at 3000 m altitude, 15.1 air-to-fuel ratio and 65% rated power setting during the cruise phase. Additionally, some studies were made about the thermodynamic optimization of engine, flight cycle analysis and the effect of energy losses on the design of engine and aircraft. Bejan and Siems [16] determined the requirements for exergy analysis and thermodynamic optimization in aircraft development. They outlined a newly emerging body of work that relied on exergy analysis and thermodynamic optimization in the design of energy systems for modern aircrafts. The minimization of exergy destruction brought the design as closely as permissible to the ideal limit. A key problem was the extraction of maximum exergy from a hot gaseous stream that was gradually

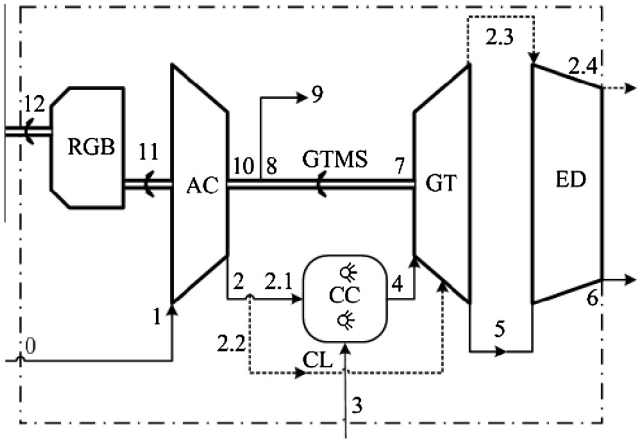

Fig. 1. A schematic of the investigated TPE.

cooled and eventually discharged into the ambient. Tona et al. [17] analyzed a turbofan engine during a typical commercial flight with exergy and thermodynamic analysis methods. This study presented the values of the exergy efficiency over the whole flight cycle, the critical equipment and the flight phases considering the exergy destruction and estimating the internal and exhaust costs. The purpose of Rigging's [18] study was to illustrate general aerospace jet engine performance (as measured by engine specific impulse and specific thrust) in terms of fundamental thermodynamic drivers, and to discuss the impacts of thermodynamic losses on the engine design, the aircraft design and their optimization.

The main objectives of this contribution are to (i) derive the energy and exergy balance relations for the T56 turboprop engine and its components, and (ii) to evaluate the performance of this system for different power loads (operation modes) using some energetic and exergetic parameters.

2. Thermodynamic analysis

Energy analysis is simply an expression of the conservation of energy stated as energy can be neither created nor destroyed. It asserts that energy is a thermodynamic property and that during an interaction, energy can be change from one form to another but the total amount of energy remains constant. However, it provides no information about the direction, in which processes can spontaneously occur, that is, the irreversibility aspects of thermodynamic processes. Exergy analysis asserts that energy has quality as well as quantity, and actual processes occur in the direction of decreasing quality of energy. The attempts to quantify the quality or "work potential" of energy in the light of the exergy analysis has caused the definition of properties entropy and exergy [19].

2.1. Energy analysis

2.1.1. Energy balance equation

Energy balance for any control volume at steady state can expressed as:

$$\dot{Q} - \dot{W} + \sum_{in} \dot{E}_{in} - \sum_{out} \dot{E}_{out} = 0 \tag{1}$$

where $\dot{Q}$ and $\dot{W}$ are the net rates of energy transfer by heat and work. The $\dot{E}$ represents the energy rate of inlet and outlet stream [20].

2.1.2. Governing equations and energy efficiency

To model this system, mass and energy balance equation were applied to the basic component in the T56 turboprop engine considering them as a control volume at steady-state. The values of enthalpy, heat energy rate, work rate in the inlet stream and outlet stream of each component were calculated with the governing equations. The governing equations for the compressor, the combustion chamber, the gas turbine and other components are given as the following [21,22]:

- Air compressor (*AC*):

$$T_{out} = T_{in}\left\{1 + \frac{1}{\eta_{AC}}\left[\left(\frac{P_{out}}{P_{in}}\right)^{\frac{\mu_a - 1}{\mu_a}} - 1\right]\right\} \tag{1}$$

$$\dot{m}_{in} = \dot{m}_{out} = \dot{m}_a \tag{2}$$

$$\dot{W}_{AC} = \dot{m}_a(c_{P,a,out}T_{out} - c_{P,a,in}T_{in}) \tag{3}$$

$$\mu_a = \frac{1}{1 - \frac{R_a}{c_{P,a}}} \tag{4}$$

$$c_{P,a}(T) = 1.04841 - \left(\frac{3.83719T}{10^4}\right) + \left(\frac{9.45378T^2}{10^7}\right) - \left(\frac{5.49031T^3}{10^{10}}\right) + \left(\frac{7.92981T^4}{10^{14}}\right) \tag{5}$$

where $c_{P,a}$, $\dot{m}_a$, P, R_a, T, $\dot{W}_{AC}$, η_{AC} and μ_a are the specific heat capacity of air, the air mass flow, the pressure, the universal gas constant of air, the temperature, the compressor work rate, the compressor isentropic efficiency and the specific heat ratio of air, respectively.

- Combustion chamber (*CC*):

$$\dot{m}_{in} \cdot c_{P,a,in}T_{in} + \eta_{CC}\dot{m}_f \cdot LHV = \dot{m}_g c_{P,g}T_{out} \tag{6}$$

$$\dot{m}_{in} + \dot{m}_f = \dot{m}_g \tag{7}$$

Table 1
Main property of the measurement devices at the test cell.

Tag number	Type/model of device	Accuracy (%)	Operating range	Unit	Uncertainty
$P_{0,1,2.3,2.4,5,6}$	331i/BOURDON	0.1	88–111.75	(kPa)	±0.10
$P_{2,2.1,2.2,4}$	331//BOURDON	0.3	0–2068.38	(kPa)	±1.50
P_3	331//BOURDON	0.1	0–689.46	(kPa)	±0.50
$T_{0,1,3}$	PT-100/MESCON	0.1	233.15–313.15	(K)	±0.25
$T_{2,2.1,2.2}$	T/C-K/MESCON	0.5	273.15–773.15	(K)	±1.05
T_4	T/C-K/MESCON	0.6	273.15–1643.15	(K)	±1.50
$T_{2.3,2.4,5,6}$	T/C-K/MESCON	0.5	273.15–973.15	(K)	±1.25
Dyno torque	F633A model/FROUDE	0.25	0–36,100	(lbf)	±12.5
Xact torque	F633A model/FROUDE	0.25	0–500	(Nm)	±1.2
RPM	M13203000/MAGNUS	0.03	0–16833	(*RPM*)	±5.5
Fuel flow	Cox AN-8 flow meter	0.3	0–0.6	(kg/s)	±0.001
Air flow	ASME flow nozzles	0.4	0–20	(kg/s)	±0.015

Table 2
Constants of combustion reaction and specific heat capacity of combustion gaseous at various operation modes.

Constants	Operation modes			
	75%	100%	MIL	Takeoff
Air–fuel ratio	56.49	45.15	42.96	41.88
ξ_1	329.91	263.70	250.90	244.57
ξ_2	12.10	12.08	12.08	12.07
ξ_3	17.77	16.51	16.27	16.15
ξ_4	50.18	36.55	33.91	32.61
ξ_5	255.61	204.32	194.40	189.49
λ_1	0.91543	0.91470	0.91451	0.91441
λ_2	0.01163	0.01280	0.01310	0.01326
λ_3	0.01529	0.01477	0.01464	0.01458
λ_4	−0.06675	−0.06581	−0.06557	−0.06545

where $c_{P,g}$, $\dot{m}_f$, $\dot{m}_g$, LHV and η_{CC} are the specific heat capacity of combustion gaseous, the fuel mass flow, the combustion gaseous mass flow, the low heating value of fuel and the energy efficiency of combustion, respectively.

- Gas turbine (GT):

$$T_{out} = T_{in}\left\{1 - \eta_{GT}\left[1 - \left(\frac{P_{in}}{P_{out}}\right)^{\frac{1-\mu_g}{\mu_g}}\right]\right\} \tag{8}$$

$$\dot{m}_{in} = \dot{m}_{out} = \dot{m}_g \tag{9}$$

$$\dot{W}_{GT} = \dot{m}_g(c_{P,g,in,}T_{in} - c_{P,g,out}T_{out}) \tag{10}$$

$$\mu_g = \frac{1}{1 - \frac{R_g}{c_{P,g}}} \tag{11}$$

where R_g, $\dot{W}_{GT}$, η_{GT} and μ_g are the universal gas constant of combustion gaseous, the turbine work rate, the turbine isentropic efficiency and the specific heat ratio of combustion gaseous.

- Exhaust duct (ED):

$$\dot{Q}_{out} = \eta_{ED}\dot{Q}_{in} \tag{12}$$

- Gas turbine mechanical shaft ($GTMS$):

$$\dot{W}_{AC} + \dot{W}_{RGB,in} = (\eta_{GTMS}\dot{W}_{GT} - \dot{W}_{Acc}) \tag{13}$$

- Reduction gearbox (RGB):

$$\dot{W}_{\mathrm{Pr},TPE} = \eta_{RGB}\dot{W}_{RGB,in} \tag{14}$$

where $\dot{Q}, \dot{W}_{Acc}, \dot{W}_{RGB}, \dot{W}_{\mathrm{Pr},TPE}$, η_{ED} η_{GTMS} and η_{RGB} represent the heat rate, the work rate utilized by accessory group, the reduction gearbox inlet shaft work rate, the net product work rate of turboprop engine, the energy efficiency of ED, the mechanical efficiency of $GTMS$ and RGB, respectively.

In this study, all performance assessment of the T56 turboprop engine were made according to the shaft power (named as Case A) and the shaft power plus the kinetic energy (or exergy) rate of exhaust gaseous (named as Case B) because the energy and exergy of exhaust gaseous were considered.

- For Case A:

$$\eta_{TPE} = \frac{\dot{W}_{\mathrm{Pr}}}{\dot{m}_f LHV} \tag{15}$$

- For Case B:

$$\eta_{TPE} = \frac{\dot{W}_{\mathrm{Pr},TPE} + \dot{E}_{kn}}{\dot{m}_f LHV} \tag{16}$$

where η_{TPE} is the energy efficiency of the T56 turboprop engine, $\dot{E}_{kn}$ is the kinetic energy rate of exhaust gaseous.

2.2. Exergy analysis

Exergy analysis is a method that uses the conservation of mass and conservation of energy principles together with the second law of thermodynamics for the analysis, design and improvement of energy and other systems.

2.2.1. Exergy balance equation and exergy terms

Exergy balance for any control volume at steady state is given as [20,21]:

$$\sum\left(1 - \frac{T_o}{T_k}\right)\dot{Q}_k - \dot{W} + \sum_{in}\dot{E}x_{in} - \sum_{out}\dot{E}x_{out} - \dot{E}x_D = 0 \tag{17}$$

where $\dot{Q}_k$ is the heat transfer rate through the boundary at temperature T_k at location k, $\dot{W}$ is the work rate, $\dot{E}x$ is the exergy rate of inlet and olutlet stream, and $\dot{E}x_D$ is the exergy destruction rate. In the absence of nuclear, magnetism, electricity and surface tension effects in the thermal systems, the total exergy for a flow of matter through a system can be determined from:

$$\dot{E}x = \dot{m}(\varepsilon_{kn} + \varepsilon_{pt} + \varepsilon_{ph} + \varepsilon_{ch}) \tag{18}$$

where ε_{kn}, ε_{pt}, ε_{ph} and ε_{ch} denote the specific kinetic exergy, specific potential exergy, specific physical exergy and specific chemical exergy, respectively. In this study, the changes in the kinetic exergy and potential exergy within the T56 turboprop engine were assumed to be negligible. According to the ideal gas expression, the specific physical exergy for air and combustion gaseous with constant specific heat capacity may be written as [20]:

$$\varepsilon_{ph} = c_{P(T)}\left[T - T_o - T_o\ln\left(\frac{T}{T_o}\right)\right] + RT_o\ln\left(\frac{P}{P_o}\right) \tag{19}$$

The specific chemical exergy of liquid fuels ($C_xH_yO_zS_\sigma$) on a unit mass can be determined as flows [11,23,24]:

$$\frac{\varepsilon_{ch,f}}{LHV} = \gamma_f \cong 1.0401 + 0.01728\frac{y}{x} + 0.0432\frac{z}{x} + 0.2196\frac{\sigma}{x}\left(1 - 2.0628\frac{y}{x}\right) \tag{20}$$

where γ_f denotes the fuel exergy grade function that is estimated to be 1.06789 for kerosene of type JP-8 jet fuel.

2.2.2. Exergy efficiency terms

Exergy efficiency equations of basic components of the T56 turboprop engine are defined as follows:

- Air compressor (AC):

$$\psi_{AC} = \frac{\dot{E}x_{out} - \dot{E}x_{in}}{\dot{W}_{AC}} \tag{21}$$

- Combustion chamber (CC):

$$\psi_{CC} = \frac{\dot{E}x_{out}}{\dot{E}x_{in}} = \frac{\dot{E}x_{out,g}}{\dot{m}_f.\varepsilon_{ch} + \dot{E}x_{in,a}} \tag{22}$$

- Gas turbine (GT):

$$\psi_{GT} = \frac{\dot{W}_{GT}}{\dot{E}x_{in} - \dot{E}x_{out}} \tag{23}$$

Table 3
Main measurement data and performance parameters of the whole *TPE* at Cases A and B.

Parameter	Unit	Case	Operation modes			
			0.75%	100%	MIL	Takeoff
$\dot{m}_f$	(kg/s)	A, B	0.235	0.294	0.309	0.317
$\dot{E}_f$	(kW)	A, B	10058.0	12583.2	13225.2	13567.6
$\dot{E}x_f$	(kW)	A, B	10740.9	13437.5	14123.1	14488.7
$\dot{W}_{12,TPE}$	(kW)	A, B	2198.7	2996.3	3256.3	3442.0
F	(lbf)	B	688.0	735.6	746.1	750.0
V	(m/s)	B	204.2	217.5	220.4	221.4
$\dot{E}, \dot{E}x_{kn,TPE}$	(kW)	B	312.5	355.8	365.7	369.3
$E\dot{S}P$	(kW)	B	2511.2	3352.1	3621.9	3811.3
SFC	(kg/kW h)	A	0.385	0.353	0.342	0.332
		B	0.337	0.316	0.307	0.299
$\dot{E}_{L,TPE}$	(kW)	A	7859.3	9586.9	9968.9	10125.6
		B	7546.8	9231.1	9603.3	9756.3
$\dot{E}_{C,TPE}$	(kW)	A	8542.2	10441.2	10866.8	11046.7
		B	8229.7	10085.5	10501.2	10677.4
η_{TPE}	(%)	A	21.9	23.8	24.6	25.4
		B	25.0	26.6	27.4	28.1
ϕ_{TPE}	(%)	A	78.1	76.2	75.4	74.6
		B	75.0	73.4	72.6	71.9
φ_{TPE}	(%)	A	357.5	320.0	306.1	294.2
		B	300.5	275.4	265.1	256.0
$\dot{E}IP_{TPE}$	(kW)	A	6141.2	7304.1	7514.4	7556.8
		B	5662.6	6772.1	6973.3	7015.6
$FPR_{en,TPE}$	(–)	A	4.6	4.2	4.1	3.9
		B	4.0	3.8	3.7	3.6
ψ_{TPE}	(%)	A	20.5	22.3	23.1	23.8
		B	23.4	24.9	25.6	26.3
α_{TPE}	(%)	A	79.5	77.7	76.9	76.2
		B	76.6	75.1	74.4	73.7
β_{TPE}	(%)	A	388.5	348.5	333.7	320.9
		B	327.7	300.9	289.9	280.1
$\dot{E}xIP_{TPE}$	(kW)	A	6793.6	8113.1	8361.4	8422.4
		B	6305.6	7569.6	7808.1	7868.7
$FPR_{ex,TPE}$	(–)	A	4.9	4.5	4.3	4.2
		B	4.3	4.0	3.9	3.8

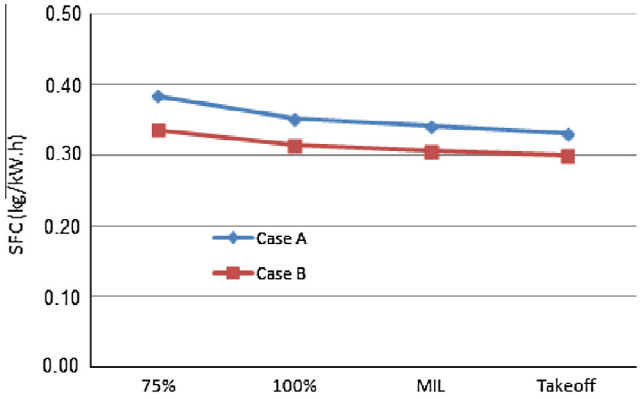

Fig. 2. The specific fuel consumption (SFC) of the engine at different operation modes.

- Exhaust duct (*ED*):

$$\psi_{ED} = \frac{\dot{E}x_{out}}{\dot{E}x_{in}} \tag{24}$$

- Gas turbine mechanical shaft (*GTMS*):

$$\psi_{GTMS} = \frac{(\dot{W}_{ACC} + \dot{W}_{Acc} + \dot{W}_{RGB,in})}{\dot{W}_{GT}} \tag{25}$$

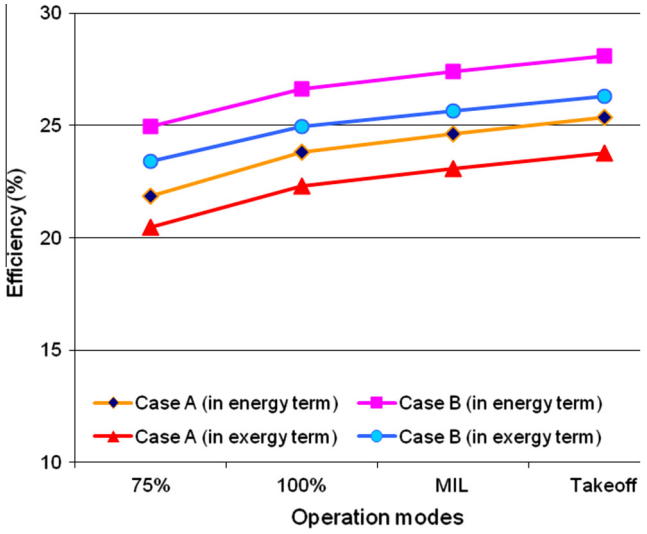

Fig. 3. Efficiency values of the T56 turboprop engine at different operation modes.

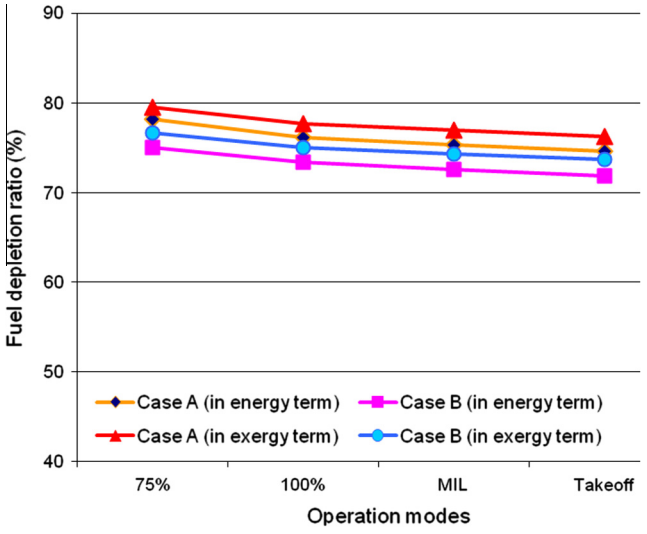

Fig. 4. Fuel depletion ratio of the T56 turboprop engine at different operation modes.

- Reduction gearbox (RGB):

$$\psi_{RGB} = \frac{\dot{W}_{Pr,TPE}}{\dot{W}_{RGB,in}} \tag{26}$$

- T56 turboprop engine (*TPE*) for Case A:

$$\psi_{TPE} = \frac{\dot{W}_{Pr,TPE}}{\dot{m}_f \varepsilon_{ch,f}} \tag{27}$$

- T56 turboprop engine (*TPE*) for Case B:

$$\psi_{TPE} = \frac{\dot{W}_{Pr,TPE} + \dot{E}x_{kn}}{\dot{m}_f \varepsilon_{ch,f}} \tag{28}$$

where ψ and $\dot{E}x_{kn}$ state the exergy efficiency and the kinetic exergy rate of exhaust gaseous.

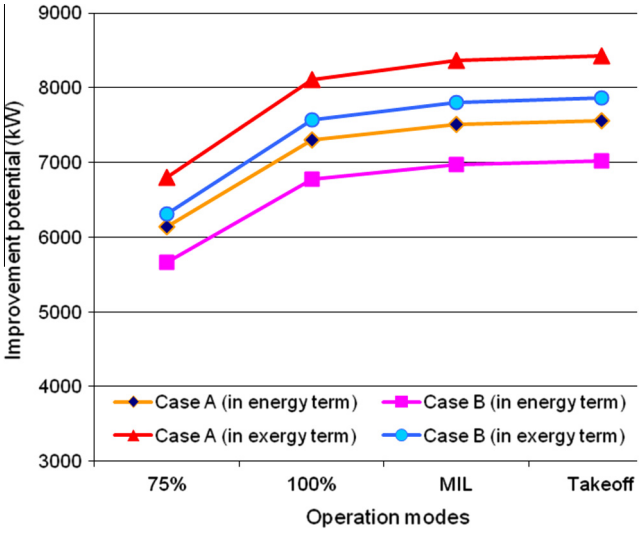

Fig. 5. Improvement potential of the thermodynamic inefficiencies at different operation modes.

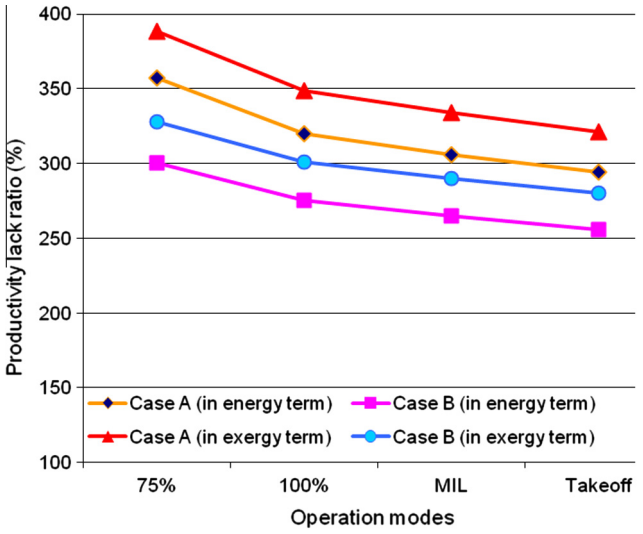

Fig. 6. Productivity lack ratio of the *TPE* at different operation modes.

2.3. Performance parameters

2.3.1. Specific fuel consumption

SFC is the mass of fuel burnt per unit time of total output power. It is essential for minimizing the *SFC* for applications where the weight or/and cost of fuel are significant. When specifying the SFC values, it is also important to state whether the lower or higher calorific value of the fuel is used. For the turboprop engine, the *SFC* is obtained from:

$$SFC = \frac{\dot{m}_f}{\dot{E}SP} \tag{29}$$

where $\dot{E}SP$ states the equivalent shaft power. The $\dot{E}SP$ consists of the net shaft power and the equivalent power (kinetic energy/exergy rate) of exhaust gaseous. Residual thrust of the T56 turboprop engine can be calculated from [8]:

$$F = \dot{m}_{out}V_{out} - \dot{m}_{in}V_{in} + A_{out}P_{out} - A_{in}P_{in} \tag{30}$$

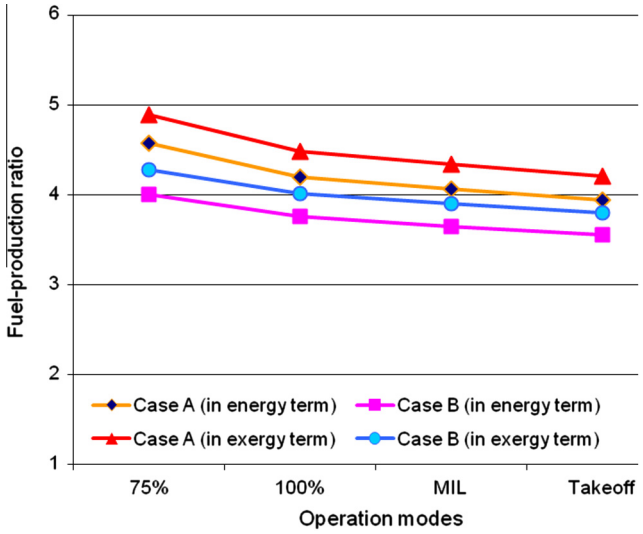

Fig. 7. Fuel-production ratio of the *TPE* at different operation modes.

where *A*, *F* and *V* are the area of inlet and outlet of engine components, the residual thrust and the velocity of inlet and outlet streams. Incoming momentum is assumed as zero ($V_{in} \cong 0$) due to the engine is being operated in a ground test cell. When the residual thrust is known, the velocity of stream can be estimated from Eq. (30). The kinetic energy or exergy of the residual thrust is given by [12]:

$$\dot{E}_{kn} = \dot{E}x_{kn} = \dot{m}_g \frac{V_{out}^2}{2000} \tag{31}$$

The $\dot{E}SP$ of the turboprop engine is determined by:

$$\dot{E}SP = \dot{W}_{\mathrm{Pr}} + \dot{E}_{kn} \tag{32}$$

where $\dot{E}SP, \dot{E}x_{kn}$ and $\dot{W}_{\mathrm{Pr}}$ are evaluated in kW.

2.3.2. Other assessment parameters

Several assessment parameters, such as the relative exergy destruction, the fuel exergy depletion rate and the productivity lack, are useful for evaluating the exergetic performance of an investigated system. These are given as follows [8,11,20,24]:

- The fuel exergy depletion (α) can be defined as the ratio of the exergy consumption (losses and destruction) for the *j*'th component to the total fuel exergy rate entering the engine. It is obtained by:

$$\alpha_j = \frac{\dot{E}x_{C,j}}{\dot{E}x_f} = \frac{\dot{E}x_{D,j} + \dot{E}x_{L,j}}{\dot{E}x_f} \tag{33}$$

- The productivity lack (β) is expressed as the ratio of the exergy consumption of the *j*'th component to the total product exergy rate of the engine. It is given as follows:

$$\beta_j = \frac{\dot{E}x_{C,j}}{\dot{E}x_{\mathrm{Pr},TPE}} = \frac{\dot{E}x_{D,j} + \dot{E}x_{L,j}}{\dot{E}x_{\mathrm{Pr},TPE}} \tag{34}$$

- The relative exergy consumption (χ) is described as the ratio of the exergy consumption of the *j*'th component to the total exergy consumption in the engine. It is estimated from:

$$\chi_j = \frac{\dot{E}x_{C,j}}{\dot{E}x_{C,TPE}} = \frac{\dot{E}x_{D,j} + \dot{E}x_{L,j}}{\dot{E}x_{C,TPE}} \tag{35}$$

Table 4
Energy rate, exergy rate and other thermodynamic properties of the *TPE* at 75%-mode.

State No.	Fluid type/work	Mass flow rate $\dot{m}$ (kg s^{-1})	Temperature $T(K)$	Pressure P (kPa)	Energy rate $\dot{E}$ (kW)	Exergy rate $\dot{E}x$ (kW)
0	Air	0.000	298.15	93.60	0.00	0.00
1	Air	14.750	298.15	93.60	0.00	0.00
2	Air	14.750	602.25	884.52	4917.84	4299.01
2.1	Air	13.275	602.25	884.52	4418.82	3869.11
2.2	Cooling air	1.475	602.25	884.52	490.98	429.90
2.3	Cooling air	1.475	741.00	95.35	742.86	269.94
2.4	Cooling air	1.475	737.30	94.87	735.96	271.94
3	Fuel	0.235	298.15	220.64	10058.00	10740.87
4	Combustion gases	13.510	1165.15	857.98	14103.83	9763.68
5	Combustion gases	13.510	741.00	95.35	6551.00	2472.69
6	Combustion gases	13.510	737.30	94.87	6489.42	2433.25
7	Shaft power				7301.75	7301.75
8	Shaft power				7191.78	7191.78
9	Shaft power				41.76	41.76
10	Shaft power				7150.02	7150.02
11	Shaft power				2232.18	2232.18
12	Shaft power				2198.70	2198.70

Table 5
Energy rate, exergy rate and other thermodynamic properties of the *TPE* at 100%-mode.

State No.	Fluid type/work	Mass flow rate $\dot{m}$ (kg s^{-1})	Temperature T (K)	Pressure P (kPa)	Energy rate $\dot{E}$ (kW)	Exergy rate $\dot{E}x$ (kW)
0	Air	0.000	298.15	93.60	0.00	0.00
1	Air	14.750	298.15	93.60	0.00	0.00
2	Air	14.750	602.25	884.52	4917.84	4299.01
2.1	Air	13.275	602.25	884.52	4418.82	3869.11
2.2	Cooling air	1.475	602.25	884.52	490.98	429.90
2.3	Cooling air	1.475	823.40	95.35	898.47	357.65
2.4	Cooling air	1.475	819.28	94.87	890.60	359.03
3	Fuel	0.294	298.15	220.64	12583.20	13437.51
4	Combustion gases	13.569	1285.15	857.98	16571.08	11453.09
5	Combustion gases	13.569	823.40	95.35	8040.76	3290.40
6	Combustion gases	13.569	819.28	94.87	7969.38	3243.06
7	Shaft power				8123.63	8123.63
8	Shaft power				8001.51	8001.51
9	Shaft power				41.76	41.76
10	Shaft power				7959.75	7959.75
11	Shaft power				3041.91	3041.91
12	Shaft power				2996.28	2996.28

Table 6
Energy rate, exergy rate and other thermodynamic properties of the *TPE* at MIL-mode.

State No.	Fluid type/work	Mass flow rate $\dot{m}$ (kg s^{-1})	Temperature T (K)	Pressure P (kPa)	Energy rate $\dot{E}$ (kW)	Exergy rate $\dot{E}x$ (kW)
0	Air	0.000	298.15	93.60	0.00	0.00
1	Air	14.750	298.15	93.60	0.00	0.00
2	Air	14.750	602.25	884.52	4917.84	4299.01
2.1	Air	13.275	602.25	884.52	4418.82	3869.11
2.2	Cooling air	1.475	602.25	884.52	490.98	429.90
2.3	Cooling air	1.475	840.45	95.35	931.12	377.45
2.4	Cooling air	1.475	836.25	94.87	923.06	378.02
3	Fuel	0.309	298.15	220.64	13225.20	14123.10
4	Combustion gases	13.584	1315.15	857.98	17207.93	11896.92
5	Combustion gases	15.059	840.45	95.35	9286.90	3476.31
6	Combustion gases	16.534	836.25	94.87	10106.91	3427.18
7	Shaft power				8391.34	8391.34
8	Shaft power				8265.45	8265.45
9	Shaft power				41.76	41.76
10	Shaft power				8223.69	8223.69
11	Shaft power				3305.85	3305.85
12	Shaft power				3256.26	3256.26

- The maximum improvement in the exergy efficiency for a process or system can be achieved when the exergy consumption (losses and destruction) is minimized. The exergetic improvement potential ($\dot{E}xIP$) of the j'th component may be written as follows:

$$\dot{E}x\dot{I}P_j = (1-\psi)(\dot{E}x_D + \dot{E}x_L)_j \tag{36}$$

These assessment parameters may be written with the energetic terms as follows [20]:

Table 7
Energy rate, exergy rate and other thermodynamic properties of the *TPE* at Takeoff-mode.

State No.	Fluid type/work	Mass flow rate $\dot{m}$ (kg s^{-1})	Temperature T (K)	Pressure P (kPa)	Energy rate $\dot{E}$ (kW)	Exergy rate $\dot{E}x$ (kW)
0	Air	0.000	298.15	93.60	0.00	0.00
1	Air	14.750	298.15	93.60	0.00	0.00
2	Air	14.750	602.25	884.52	4917.84	4299.01
2.1	Air	13.275	602.25	884.52	4418.82	3869.11
2.2	Cooling air	1.475	602.25	884.52	490.98	429.90
2.3	Cooling air	1.475	847.00	95.35	943.69	384.80
2.4	Cooling air	1.475	842.77	94.87	935.56	385.40
3	Fuel	0.317	298.15	220.64	13567.60	14488.75
4	Combustion gases	13.592	1330.22	857.98	17532.03	12123.73
5	Combustion gases	15.067	847.00	95.35	9419.37	3546.16
6	Combustion gases	16.542	842.77	94.87	10250.92	3496.38
7	Shaft power				8582.87	8582.87
8	Shaft power				8454.03	8454.03
9	Shaft power				41.76	41.76
10	Shaft power				8412.27	8412.27
11	Shaft power				3494.43	3494.43
12	Shaft power				3442.01	3442.01

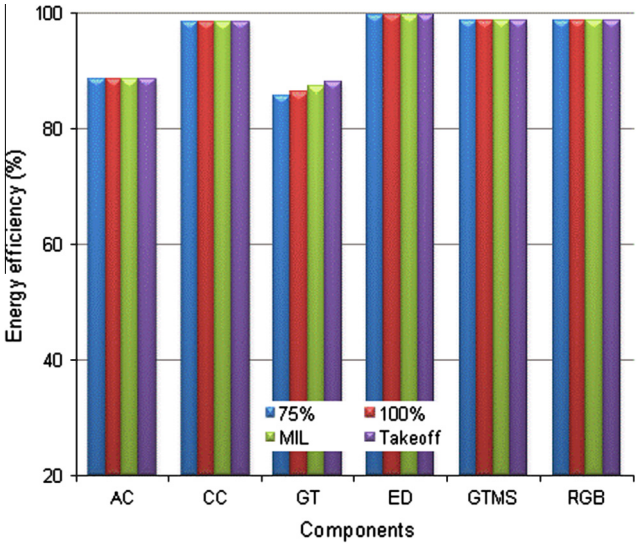

Fig. 8. Energy efficiency of the *TPE* components at different operation modes.

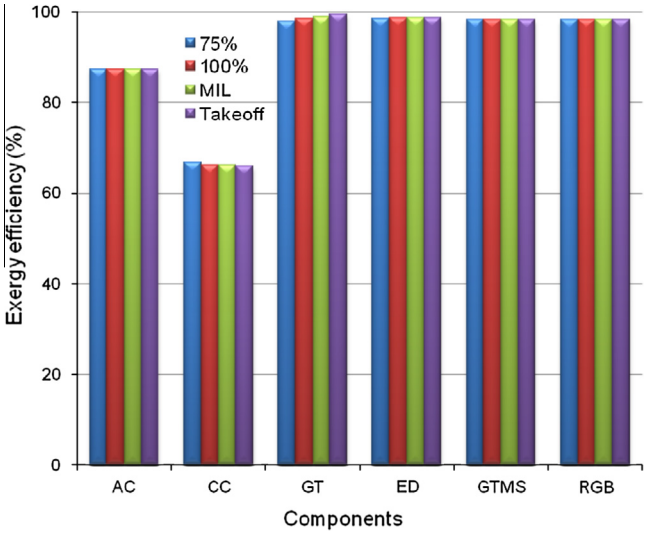

Fig. 9. Exergy efficiency values of the *TPE* components at various operation modes.

- The fuel energy depletion ratio (ϕ):

$$\phi_j = \frac{\dot{E}_{L,j}}{\dot{E}_f} \tag{37}$$

- The productivity lack ratio (φ):

$$\varphi_j = \frac{\dot{E}_{L,j}}{\dot{E}_{\mathrm{Pr},TPE}} \tag{38}$$

- The relative energy loss ratio (θ):

$$\theta_j = \frac{\dot{E}_{L,j}}{\dot{E}_{L,TPE}} \tag{39}$$

- The energetic improvement potential rate ($\dot{E}IP$):

$$\dot{E}IP_j = (1-\eta)\dot{E}_{L,j} \tag{40}$$

2.3.3. Energetic and exergetic fuel-production ratios (FPR_{en} and FPR_{ex})

Energetic fuel-production ratio (FPR_{en}) is defined as the ratio of total fuel energy rate consumed by the engine to the total power produced by the engine. The FPR_{en} is estimated from:

$$FPR_{en,TPE} = \frac{\dot{E}_{f,TPE}}{\dot{E}_{\mathrm{Pr},TPE}} \tag{41}$$

Exergetic fuel-production ratio (FPR_{ex}) is explained as the ratio of total fuel exergy rate consumed by the engine to total power produced by the engine. The FPR_{ex} is calculated from:

$$FPR_{ex,TPE} = \frac{\dot{E}x_{f,TPE}}{\dot{E}x_{\mathrm{Pr},TPE}} \tag{42}$$

The *FPR* is an important parameter to compare the thermal systems. The more *FPR* approaches to 1 the more the system efficiency increases. When the *FPR* is equal to 1, the system efficiency becomes 100% and it can be assumed as an ideal system. This parameter is preferred and used for the first time in this study to the best of the authors' knowledge.

3. An application for the T56 turboprop engine (TPE)

3.1. General description of the TPE

The T56 turboprop engines (*TPE*) have been used on Lockheed Martin's C-130 Hercules tactical transport aircrafts in Turkish Air Forces. A schematic of *TPE* investigated is illustrated in Fig. 1. The

Table 8
Exergy rate, exergetic efficiency and other thermodynamic parameters of the engine components at 75%-mode (Case A: A and Case B: B).

Component	$\dot{E}x_{in}$ (kW)	$\dot{E}x_{out}$ (kW)	$\dot{E}x_C$ (kW)	ψ (%)	ϕ (%)	φ (%)		θ (%)		$Ex\dot{I}P$ (kW)
						A	B	A	B	
AC	4917.84	4299.01	618.83	87.42	5.76	28.15	24.64	7.24	7.52	77.87
CC	14609.98	9763.68	4846.29	66.83	45.12	220.42	192.99	56.73	58.89	1607.57
GT	7450.96	7301.75	149.21	98.00	1.39	6.79	5.94	1.75	1.81	2.99
ED	2742.63	2705.19	37.44	98.64	0.35	1.70	1.49	0.44	0.45	0.51
GTMS	7301.75	7191.78	109.97	98.49	1.02	5.00	4.38	1.29	1.34	1.66
RGB	2232.18	2198.70	33.48	98.50	0.31	1.52	1.33	0.39	0.41	0.50

Table 9
Exergy rate, exergetic efficiency and other thermodynamic parameters of the engine components at 100%-mode (Case A: A and Case B: B).

Component	$\dot{E}x_{in}$ (kW)	$\dot{E}x_{out}$ (kW)	$\dot{E}x_C$ (kW)	ψ (%)	ϕ (%)	φ (%)		θ (%)		$Ex\dot{I}P$ (kW)
						A	B	A	B	
AC	4917.84	4299.01	618.83	87.42	4.61	20.65	18.46	5.93	6.14	77.87
CC	17306.62	11453.09	5853.53	66.18	43.56	195.36	174.63	56.06	58.04	1979.81
GT	8234.93	8123.63	111.30	98.65	0.83	3.71	3.32	1.07	1.10	1.50
ED	3648.06	3602.09	45.97	98.74	0.34	1.53	1.37	0.44	0.46	0.58
GTMS	8123.63	8001.51	122.13	98.50	0.91	4.08	3.64	1.17	1.21	1.84
RGB	3041.91	2996.28	45.63	98.50	0.34	1.52	1.36	0.44	0.45	0.68

Table 10
Exergy rate, exergetic efficiency and other thermodynamic parameters of the engine components at MIL-mode (Case A: A and Case B: B).

Component	$\dot{E}x_{in}$ (kW)	$\dot{E}x_{out}$ (kW)	$\dot{E}x_C$ (kW)	ψ (%)	ϕ (%)	φ (%)		θ (%)		$Ex\dot{I}P$ (kW)
						A	B	A	B	
AC	4917.84	4299.01	618.83	87.42	4.38	19.00	17.09	5.69	5.89	77.87
CC	17992.21	11896.92	6095.29	66.12	43.16	187.19	168.29	56.09	58.04	2064.92
GT	8473.06	8391.34	81.73	99.04	0.58	2.51	2.26	0.75	0.78	0.79
ED	3853.76	3805.21	48.55	98.74	0.34	1.49	1.34	0.45	0.46	0.61
GTMS	8391.34	8265.45	125.89	98.50	0.89	3.87	3.48	1.16	1.20	1.89
RGB	3305.85	3256.26	49.59	98.50	0.35	1.52	1.37	0.46	0.47	0.74

Table 11
Exergy rate, exergetic efficiency and other thermodynamic parameters of the engine components at Takeoff-mode (Case A: A and Case B: B).

Component	$\dot{E}x_{in}$ (kW)	$\dot{E}x_{out}$ (kW)	$\dot{E}x_C$ (kW)	ψ (%)	ϕ (%)	φ (%)		θ (%)		$Ex\dot{I}P$ (kW)
						A	B	A	B	
AC	4917.84	4299.01	618.83	87.42	4.27	17.98	16.24	5.60	5.80	77.87
CC	18357.85	12123.73	6234.13	66.04	43.03	181.12	163.57	56.43	58.39	2117.04
GT	8622.67	8582.87	39.80	99.54	0.27	1.16	1.04	0.36	0.37	0.18
ED	3930.96	3881.78	49.18	98.75	0.34	1.43	1.29	0.45	0.46	0.62
GTMS	8582.87	8454.03	128.84	98.50	0.89	3.74	3.38	1.17	1.21	1.93
RGB	3494.43	3442.01	52.42	98.50	0.36	1.52	1.38	0.47	0.49	0.79

TPE consists of an air compressor (*AC*), a combustion chamber (*CC*), a gas turbine (*GT*), an exhaust duct (*ED*), a reduction gearbox (*RGB*), and a gas turbine mechanical shaft (*GTMS*)

3.2. Assumptions made

In this study, the assumptions made are listed below:

- The *TPE* operated in a steady-state and steady flow.
- The principle of ideal-gas mixture was applied for the air and combustion gaseous.
- The combustion reaction was complete.
- The fuel injected to combustion chamber was the JP-8 jet fuel.
- The LHV was assumed to be 42,800 kJ/kg.
- The compressor and the gas turbine were considered adiabatic.
- The changes in the kinetic energy, the kinetic exergy, the potential energy and the potential exergy within *TPE* were assumed to be negligible.
- The velocity of air mass flow entering the engine was taken zero due to the run test was performed in a static condition at the test cell.
- The temperature and the pressure of the dead (environmental) state were measured to be 298.15 K and 93.6 kPa, respectively.
- The air composed of nitrogen 77.48%, oxygen 20.59%, carbon dioxide 0.03% and water vapor 1.90%. Other small amounts of argon, CO, etc. in the air were neglected.
- The bleed air flow used to cool the gas turbine section was assumed to be 10% of the total air flow entering the engine.

3.3. Measurement system and experimental data

The measurement data of the T56 turboprop engine were taken from the Depot Level Engine Test Cell at 1st Air Supply and Maintenance Center of Turkish Air Forces (TurAF) for T56-A-7/-17 LFE and TYNE-MK-22 model turboprop engine. The test cell was established by Magnus Engineering and Maintenance Ltd. in August

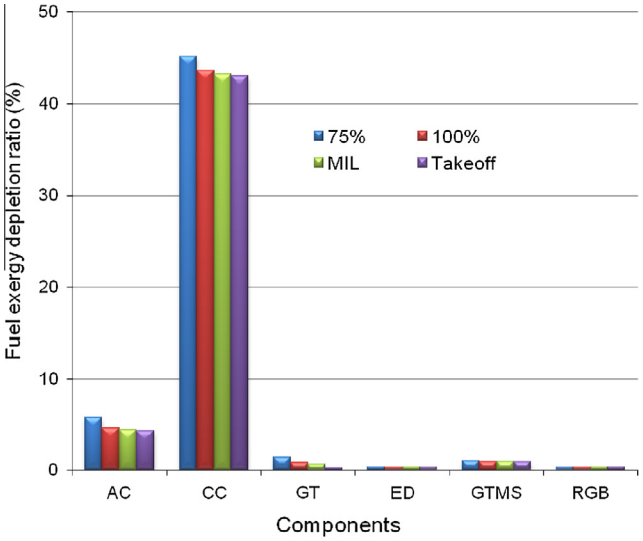

Fig. 10. Fuel exergy depletion ratio values of the *TPE* components at various operation modes.

2002. This test was performed during yearly calibration audit on September 25, 2012. In the calibration audit test, more data are measured than normal engine run test. The data measured are listed in below:

- Ambient pressure and temperature (P_o, T_o)
- Compressor inlet and outlet pressure (P_1, P_2)
- Compressor inlet and outlet temperature (T_1, T_2)
- Turbine inlet and outlet temperature (T_4, $T_{2.3,5}$)
- Turbine inlet and outlet pressure (P_4, $P_{2.3,5}$)
- Exhaust duct outlet pressure and temperature ($P_{2.4,6}$, $T_{2.4,6}$)
- Fuel flow ($\dot{m}_f$)
- Air flow ($\dot{m}_a$)
- Shaft power ($\dot{W}_{12}$)
- Residual thrust of exhaust gaseous (F)

The test cell data sheet includes the air mass flow data. The air mass flow changes with the engine speed, the ambient temperature and the pressure. The air mass flow was selected to be 14.75 kg/s. Besides, the air mass flow was measured by ASME-style flow nozzles with static pressure tabs that were pre-calibrated against NIST-traceable flow standard. The calibration and accuracy of both the devices and the test cell system are calibrated by TurAF Calibration Laboratory yearly. Air Force Metrology and Calibration Program Office (AFMETCAL, USA) is the authorized foundation to survey TurAF Calibration Laboratory biyearly. The parameter, type of the device, the operating range, the accuracy and the uncertainty of the measurements are given in Table 1.

3.4. Operation modes

There are two basic types of turboprop engines: single shaft and free turbine. The main difference between the single shaft and the free turbines is in the transmission of the power to the propeller. In the free-turbine engine, the propeller is driven by a dedicated turbine. A different turbine drives the compressor; this turbine and its compressor run at a nearly-constant speed (*RPM*) regardless of the propeller pitch and speed. Other type of the turboprop engine is the fixed-shaft constant-speed type. In this type of the engine, the ambient air is directed to the compressor section through the engine inlet. An acceleration/diffusion process in the compressor increases air pressure and directs it rearwards to a combustor. In

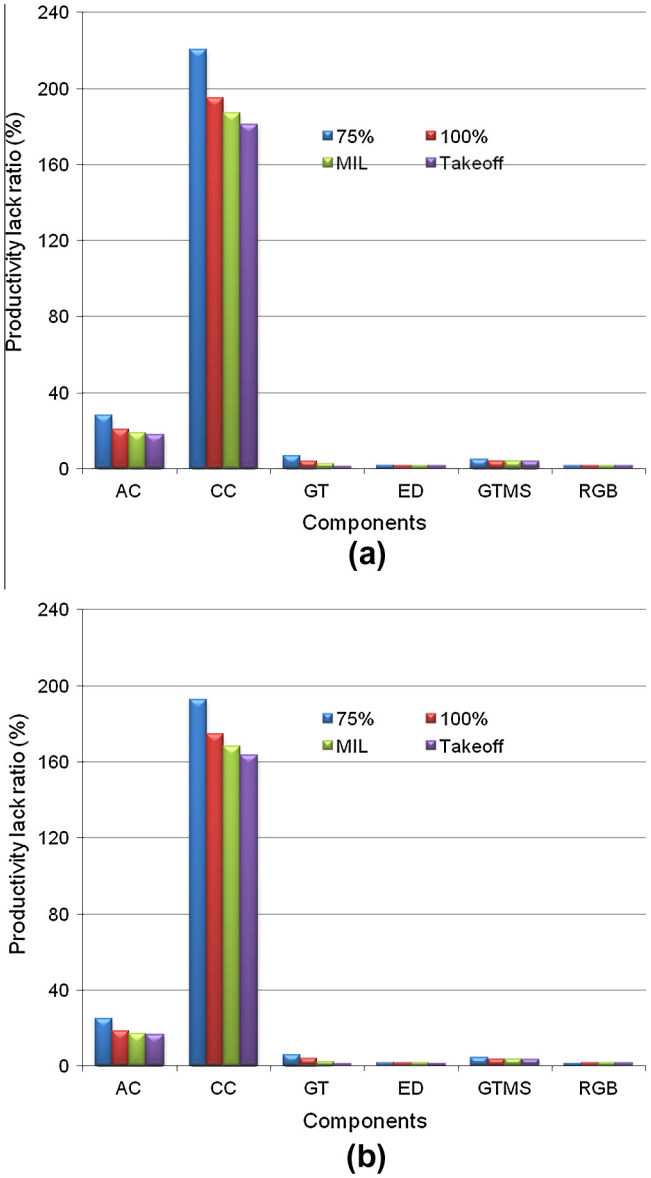

Fig. 11. Productivity lack ratio values of the *TPE* components at various operation modes: for (a) Case A and (b) Case B.

the fixed-shaft constant speed engine, the *RPM* may be varied within a narrow range of 96–100%. During the ground operation, the *RPM* may be reduced to 70%. In flight, the engine operates at a constant speed, which is maintained by governing section of propeller. Power changes are made by increasing the fuel flow and the propeller blade angle rather than the engine speed. An increase in fuel flow causes an increase in the temperature and a corresponding increase in energy available to the turbine. The turbine absorbs more energy and transmits it to the propeller in the form of torque. The increased torque forces the propeller blade angle to be increased to maintain the constant speed. Turboprop instrumentation in a fixed-shaft turboprop engine typically consists of the following basic indicators: (i) torque or horsepower, (ii) turbine inlet temperature, (iii) fuel flow and (iv) *RPM*. It is often useful and sometimes necessary for the pilot to know the shaft horse power output of the turboprop engine. Because the torque (i.e., the reaction of the complete engine to the power output) is directly proportional to the *SHP*, the measurement of the torque gives the desired information. The turboprop engine can be tested either by its propeller and propeller gearbox (*RGB*) or by a dynamometer

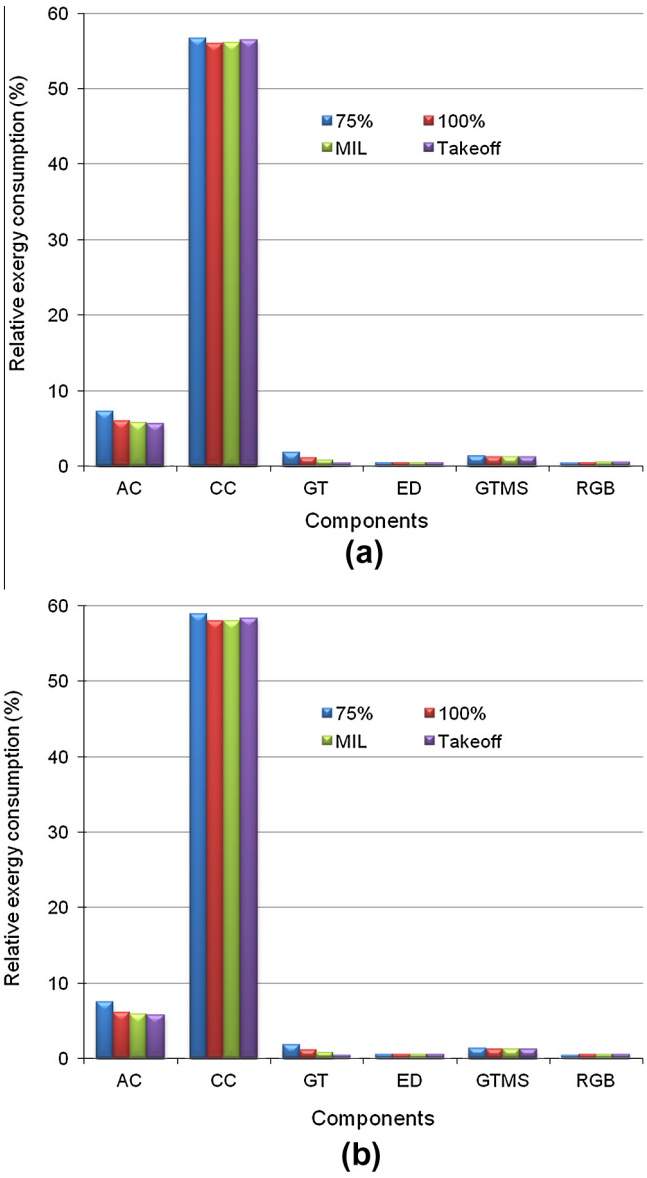

Fig. 12. Relative exergy consumption values of the *TPE* components at various operation modes: (a) Case A, (b) Case B.

instead of the propeller and the propeller gearbox in the ground test laboratory. At the test cell, the *RGB* shaft is connected to a water brake dynamometer spline, so the gas turbine mechanical shaft (*GTMS*) rotates along with the dynamometer shaft. The test operator can select the requested dynamometer torque or speed during the test [24].

The T56 turboprop engine has been investigated in this study. The T56 engine is a fixed-single shaft constant-speed type turboprop engine. While the T56 turboprop engine operated at 13,880 *RPM*-constant speed, that is maximum permissible speed, the test cell operator increased the fuel flow step by step according to the selected dynamometer torque named power loading mode. This power loading modes consisted of the 75%-mode, 100%-mode, military (MIL) mode and Takeoff mode. At the local conditions (ambient temperature: 298.2 K, pressure: 93.6 kPa), the engine shaft power was measured to be 2198.7 kW for 0.235 kg/s-fuel flow at 75%-mode, 29996.3 kW for 0.294 kg/s-fuel flow at 100%-mode, 3256.3 kW for 0.309 kg/s-fuel flow at MIL mode and 3442 kW for 0.317 kg/s-fuel flow at Takeoff mode. The turbine inlet temperature increased from 1165.15 K to 1330.22 K with the increase in the fuel flow related to the operation modes. The residual thrust was measured to be 688 lbf at 75%-mode, 735.6 lbf at 100%-mode, 746.1 lbf at MIL mode, and 750 lbf at Takeoff-mode, respectively.

3.5. Combustion balance and specific heat capacity of emissions

The air-to-fuel ratio is to be at appropriate level for enabling a stable burning. To have completed burning of the fuel and to decrease the temperature, the air-to-fuel ratio in the combustor is always higher than the stoichiometric ratio. Because of this, there is significant amount of oxygen within exhaust gaseous. The general combustion reaction equation is given as follows:

$$C_{12}H_{23} + \xi_1 \begin{pmatrix} 0.7448N_2 + \\ 0.2059O_2 + \\ 0.0003CO_2 + \\ 0.019H_2O \end{pmatrix} \rightarrow \xi_2(CO_2) + \xi_3(H_2O) + \xi_4(O_2) + \xi_5(N_2) \tag{43}$$

The specific heat capacity of the combustion gaseous can be written in the following form:

$$c_{P,cg}(T) = \lambda_1 + \frac{\lambda_2}{10^2}T + \frac{\lambda_3}{10^5}T^2 - \frac{\lambda_4}{10^9}T^3 \tag{44}$$

where the temperature is evaluated in *K*. The combustion reaction equation constants (ξ) and the specific heat capacity constants λ of the combustion gaseous were calculated for each operation mode and are summarized in Table 2.

3.6. Energy and exergy balance equations of the whole TPE

Generally, the only shaft power was taken into consideration for the turboprop and turbo shaft engines in the literature. However, considering both the shaft power and the residual power (kinetic energy/exergy value of exhaust gases) is more realistic for performing an accurate analysis. For the whole *TPE* system, two balance equations were written according to the shaft power and the shaft power plus the kinetic exergy of the exhaust gaseous. According to the considered the engine products, the exergy balance equations are given as follows:

- Energy and exergy balance equations of the engine for Case A:

$$(\dot{E}_1 + \dot{E}_3) - \dot{W}_{12} = \dot{E}_{L,TPE} \tag{45}$$

$$(\dot{E}x_1 + \dot{E}x_3) - \dot{W}_{12} = \dot{E}x_{C,TPE} \tag{46}$$

- Energy and exergy balance equations of the engine for Case B:

$$(\dot{E}_1 + \dot{E}_3) - (\dot{W}_{12} + \dot{E}_{kn,TPE}) = \dot{E}_{L,TPE} \tag{47}$$

$$(\dot{E}x_1 + \dot{E}x_3) - (\dot{W}_{12} + \dot{E}x_{kn,TPE}) = \dot{E}x_{C,TPE} \tag{48}$$

3.7. Exergy balance equations of the TPE's components

Exergy balance equations for the main components can be written as:

- Air compressor (*AC*):

$$\dot{E}x_1 + (\dot{W}_{10} - \dot{W}_{11}) - (\dot{E}x_2) = \dot{E}x_{D,AC} \tag{49}$$

- Combustion chamber (*CC*):

$$(\dot{E}x_{2.1} + \dot{E}x_3) - \dot{E}x_4 = \dot{E}x_{D,CC} \tag{50}$$

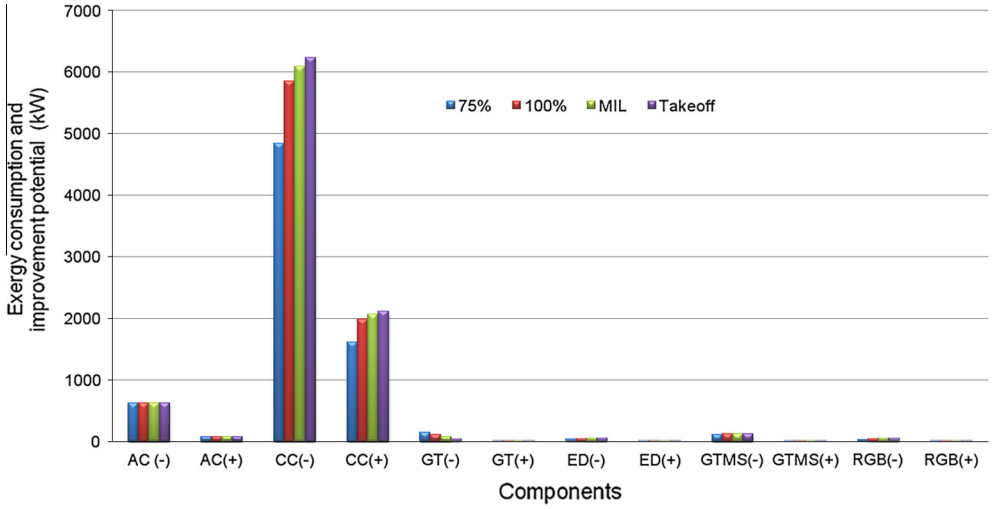

Fig. 13. Exergy consumption and its improvement potential of the *TPE* components at various operation modes (−: consumption, +: improvement potential).

Table 12
Comparing the exergetic efficiency values of the T56 and the CT7-9C turboprop engines for the maximum shaft power.

Component	ψ (%)	
	T56 turboprop engine [this study]	CT7-9C turboprop engine [13]
Compressor (AC)	87.42	90.6
Combustion chamber (CC)	66.04	79.9
Gas turbine (GT)	99.54	96.2
Power turbine (PT)	No PT	95.2
Exhaust duct (ED)	98.75	98.1
Whole engine	23.8 (for 3442 kW-shaft power)	30.0 (for 1400-kW-shaft power)

- Gas turbine (*GT*):

$$(\dot{E}x_{2.2} - \dot{E}x_{2.3}) + (\dot{E}x_4 - \dot{E}x_5) - \dot{W}_{GT} = \dot{E}x_{D,GT} \quad (51)$$

- Exhaust duct (*ED*):

$$(\dot{E}x_{2.3} - \dot{E}x_{2.4}) + (\dot{E}x_5 - \dot{E}x_6) = \dot{E}x_{D,ED} \quad (52)$$

- Gas turbine mechanical shaft (*GTMS*):

$$\dot{W}_7 - \dot{W}_8 = \dot{E}x_{D,GTMS} \quad (53)$$

$$\dot{W}_{10} = \dot{W}_8 + \dot{W}_9 \quad (54)$$

$$\dot{W}_{11} = \dot{W}_{10} - \dot{W}_{AC} \quad (55)$$

- Reduction gearbox or dynamometer (*RGB*):

$$\dot{W}_{11} - \dot{W}_{12} = \dot{E}x_{D,RGB} \quad (56)$$

$$\dot{W}_{12} = \dot{W}_{Pr,TPE} \quad (57)$$

4. Results and discussion

Energy analysis was used to evaluate the thermodynamic performance of the whole *TPE*. However, the exergy analysis was carried out for the whole *TPE* along with its main components to determine the exergetic efficiency of the components, the location and the quantity of the exergy consumption (losses and destructions), the improvement potential rate of the exergy consumption.

Table 13
Uncertainty values of the parameters unchanging with operation modes.

Parameter	Unit	Nominal value *NV*	Uncertainty u_e (±)	Percentage uncertainty u_e (±%)
P_1	(kPa)	93.60	0.10	0.11
$P_{2,2.1,2.2}$	(kPa)	884.52	1.50	0.17
P_3	(kPa)	220.64	0.50	0.23
P_4	(kPa)	857.98	1.50	0.17
$P_{2.3,5}$	(kPa)	95.35	0.10	0.10
$P_{2.4,6}$	(kPa)	94.87	0.10	0.11
$T_{1,3}$	(k)	298.15	0.25	0.08
$T_{2,.2.1,2.2}$	(k)	602.25	1.05	0.17
$\dot{m}_{1.2}$	(kg/s)	14.75	0.02	0.10
$\dot{m}_{2.2}$	(kg/s)	1.48	0.00	0.20
$\dot{m}_{2.2}$	(kg/s)	13.28	0.02	0.11
$\dot{m}_1$	(kW)	4415.82	5.82	0.13
$\dot{m}_2$	(kW)	13061.16	27.30	0.21
$\dot{m}_{2.1}$	(kW)	8400.30	17.56	0.21
$\dot{m}_{2.2}$	(kW)	933.37	2.51	0.27
$\dot{m}_2$	(kW)	4260.57	12.67	0.30
$\dot{m}_{2.1}$	(kW)	3834.51	11.56	0.30
$\dot{m}_{22}$	(kW)	426.06	1.20	0.28
$\dot{W}_{AC}$	(kW)	4917.84	10.81	0.22

4.1. Energetic and exergetic analysis results of the whole TPE

The energy efficiency, the exergy efficiency, the fuel depletion ratio, the productivity lack ratio, the improvement potential rate and the fuel-production ratio were used to evaluate the performance of the *TPE*. All the performance assessments were made according to both the shaft power (named as Case A) and the shaft power plus the kinetic energy(or exergy) rates of the exhaust gaseous (named as Case B) because both the energy and exergy of the exhaust gases were considered. The main measurement data, the results of the energy and exergy analysis of the whole *TPE* are given in Table 3. The only one way of increasing the shaft power is to increase the fuel flow due to the T56 turboprop engine is a fixed-single shaft constant-speed type turboprop engine. The shaft power raised from 2198.7 kW to 3442.0 kW while the fuel flow were increased from 0.235 kg/s to 0.317 kg/s by test cell operator according to the compulsory test steps (%75, 100%, MIL and Takeoff operation modes). The effects of changing in the fuel flow as operation modes on the energetic and exergetic performance parameters of the *TPE* are shown in Figs. 2–6. The main findings of the energy and exergy analysis are summarized as follows:

Table 14
Nominal (*NV*) and uncertainty values (u_e) of the parameters changing with operation modes.

Tag No.	Unit	Operation modes							
		75%		100%		MIL		Takeoff	
		NV	u_e (±%)	*NV*	u_e (±%)	*NV*	u_e (±%)	*NV*	u_e (±%)
T_4	(k)	1165.15	0.119	1285.15	0.117	1315.15	0.114	1330.22	0.113
$T_{2.3,5}$	(k)	741.00	0.169	823.40	0.152	840.45	0.149	847.00	0.148
$T_{2.4,6}$	(k)	737.00	0.170	819.28	0.153	836.25	0.149	842.77	0.148
$\dot{m}_{3,f}$	(kg/s)	0.234	0.427	0.294	0.340	0.309	0.324	0.317	0.315
$\dot{m}_{4.5,6}$	(kg/s)	13.509	0.118	13.569	0.118	13.584	0.118	13.592	0.118
$\dot{E}_{2.3}$	(kW)	1184.44	0.266	1340.05	0.255	1372.70	0.253	1385.28	0.253
$\dot{E}_{2.4}$	(kW)	1177.00	0.285	1332.18	0.275	1364.64	0.274	1377.14	0.273
$\dot{E}_{3,f}$	(kW)	10058.00	0.489	12583.20	0.417	13225.20	0.404	13567.60	0.397
$\dot{E}_4$	(kW)	20218.56	0.169	20693.98	0.168	21296.82	0.165	21601.17	0.164
$\dot{E}_5$	(kW)	10671.77	0.208	12132.51	0.194	12444.01	0.192	12566.39	0.191
$\dot{E}_6$	(kW)	10604.57	0.209	12060.83	0.195	12370.42	0.192	12491.97	0.191
$\dot{E}x_{2.3}$	(kW)	276.33	0.316	364.25	0.308	383.41	0.306	390.85	0.305
$\dot{E}x_{2.4}$	(kW)	271.64	0.317	359.03	0.308	378.03	0.307	385.40	0.306
$\dot{E}x_{3,f}$	(kW)	10740.87	0.489	13437.51	0.417	14123.10	0.404	14488.75	0.397
$\dot{E}x_4$	(kW)	11155.88	0.279	11479.11	0.278	11906.59	0.276	12123.73	0.276
$\dot{E}x_5$	(kW)	2490.31	0.270	3298.37	0.259	3476.31	0.257	3546.16	0.257
$\dot{E}x_6$	(kW)	2447.89	0.270	3250.87	0.260	3427.21	0.258	3496.38	0.257
$\dot{W}_{GT,7}$	(kW)	7301.75	1.073	8123.63	1.068	8391.34	1.066	8582.87	1.066
$\dot{W}_8$	(kW)	7301.30	1.073	8001.51	1.068	8265.45	1.066	8454.03	1.066
$\dot{W}_{10}$	(kW)	7259.54	1.079	7959.75	1.073	8223.69	1.072	8412.27	1.071
$\dot{W}_{11}$	(kW)	2330.89	2.434	3031.10	2.105	3295.04	2.019	3494.43	1.960
$\dot{W}_{12}$	(kW)	2198.70	0.132	2996.30	0.127	3256.30	0.126	3442.01	0.131
η	(%)	21.86	0.135	23.81	0.129	24.62	0.130	25.37	0.133
ψ	(%)	20.47	0.127	22.30	0.121	23.06	0.121	23.76	0.125

- The specific fuel consumption (*SFC*) decreases with increasing the shaft power and the residual thrust of the engine. The *SFC* was calculated to be maximum with 0.385 kg/kW h at 75%-mode and minimum with 0.332 kg/kW h Takeoff mode. The variances in the SFC are shown in Fig. 2 according to the operation modes.
- Fig. 3 indicates that the energy efficiency has a minimum value of 21.9% at 75%-mode and a maximum value of 25.5% at Takeoff mode while the exergy efficiency is found to be 20.5% at 75%-mode and 23.8% at Takeoff mode for Case A, respectively. Otherwise, for Case B, the energy efficiency is calculated to be minimum value with 25% at 75%-mode and maximum value with 28.1% at Takeoff mode when the exergy efficiency was estimated to be 23.4% at 75%-mode and 26.3% at Takeoff mode, respectively.
- An increase in the energy (or exergy) efficiency decreases the energy losses and the exergy destruction due to that the fuel consumption goes down or the produced power goes up. Fig. 4 shows that the fuel depletion ratio decreases with an increase in the shaft power and the residual thrust at different operation modes. Fig. 5 illustrates that the energetic and exergetic improvement potential of the thermodynamic inefficiencies increases by increasing the energy and exergy efficiency from 75%-mode and Takeoff mode.
- Fig. 6 represents that the productivity lack ratio values decrease with the increase in the products of the *TPE* depending on the operation modes.
- The relative increase in the shaft power rate per the fuel energy consumption decreases the fuel-production ratio values of the *TPE*, as seen from Fig. 7. For Case A, the fuel-production ratio (FPR_{en}) varies from 4.6 at 75%-mode and 3.9 at Takeoff mode while the fuel-production ratio (FPR_{ex}) in the exergy term decreases from 4.9 at 75%-mode and 4.2 at Takeoff mode. For Case B, the FPR_{en} goes down from 4.0 at 75%-mode and 3.6 at Takeoff mode when the FPR_{ex} decreases from 4.3 at 75%-mode and 3.8 at Takeoff mode.

The results of the energy and exergy analyses show that an increase in fuel flow raises the efficiency and the generated shaft power per fuel consumption since the turbine inlet temperature goes up. Similarly, the fuel-production ratio indicates that the increase in the fuel flow per unit makes more effective to the engine at the shaft power production. But the engine operation time has been limited at a high turbine inlet temperature due to that it decreases the useful economic life. The operation duration of the T56 engine at Takeoff mode and MIL mode has been restricted with 5 and 30 min, respectively.

4.2. Energy and exergy analysis results of the TJE components

The stream type and the values of the mass flow rate, the pressure, the temperature, the energy rate and the exergy rate of the *TPE* streams at different four operation modes are given in Tables 4–7 accordance with their state numbers as specified in Fig. 1. The aim of the energy analysis is to determine the thermodynamic properties of the states and to calculate the *AC* work rate and its isentropic efficiency, the *GT* work rate and its isentropic efficiency, the *CC* energy efficiency, the *ED* energy efficiency, the mechanical yield efficiency of the *GTMS* and the *RGB*, and the shaft power rate of the engine. The energy rate values in Tables 4–7 were used to count the energy efficiency of the components. The energy efficiency values of the *TPE* components are illustrated in Fig. 8. The isentropic efficiency of the *AC* was found to be 88.26% that was a constant value at all operation modes. Similarly, the mechanical efficiency of the *GTMS* and the *RGB* was accounted to be 98.5% and unchanged with the operation modes. As seen in Fig. 10, the isentropic efficiency of the *GT* changed with the turbine inlet temperature (T_4). It was obtained to be between 85.72% (at Takeoff operation mode) and 87.86% (at 75%-operation mode). The energy efficiency values of the *CC* and the *ED* were estimated to be 99.41% and approximately 99.34% (minimum 99.32% at Takeoff mode and maximum 99.38% at 100%-mode).

The main target of the exergy analysis in this study is to determine the magnitudes of the exergy consumption and their exact locations within the components of the *TPE*. Using the values given in Tables 4–7, the inlet and outlet exergy rates, the exergy destruction rate, the exergetic efficiency, the fuel depletion ratio, the productivity lack ratio, the relative exergy consumption, and the exergetic improvement potential were derived for each component of the *TPE* and are listed in Tables 8–11 in accordance with operation modes. The main findings of the component-based exergy analysis are given as follows:

- The exergetic efficiencies of the *AC*, the *GTMS* and the *RGB* were calculated to be 87.42%, 98.5% and 98.5%, respectively. These values remained constant at all operation modes. The exergy efficiency of the *ED* changed with a little increase (98.64–98.74%). The exergy efficiency of the *CC* decreased from 66.83% at 75%-mode to 66.04% at Takeoff-mode by increasing the fuel consumption rate. Conversely of the *CC* efficiency, the exergy efficiency of the *GT* increased from 98% at 75%-mode to 99.54% at Takeoff-mode by increasing the turbine inlet temperature (T_4). The exergy efficiency of the components at different operation modes is shown in Fig. 9.
- The produced shaft power was measured to be 2198.7 kW at 75%-mode, 2996.28 kW at 100%-mode, 3256.26 kW at MIL-mode and 3442.01 kW at Takeoff-mode. At the same time, the fuel exergy rates consumed by the engine were calculated to be 10740.87 kW at 75%-mode, 13437.51 kW at 100%-mode, 14123.1 kW at MIL-mode and 14488.75 kW at Takeoff-mode, respectively. Because the increase in the produced shaft power was relatively higher than the increase in the fuel exergy rate, the fuel exergy depletion ratio and the productivity lack ratio decreased with increasing the fuel flow. The variations of the fuel exergy depletion and the productivity lack ratios are illustrated in Figs. 10 and 11.
- The exergy analysis demonstrates that, for the operating modes considered, the combustion chamber (*CC*) incurs the most significant exergy consumption in the turboprop engine due to the exergy destruction. The exergy consumption rates of the *CC* were obtained to be 4846.29 kW at 75%-mode, 5853.53 kW at 100%-mode, 6095.29 kW at MIL-mode and 6234.13 kW at Takeoff-mode, respectively.
- The variations in the relative exergy destruction ratio values of the components are presented in Fig. 12. The figure indicates that the relative exergy destruction ratio of the *CC* is maximum with approximately 56% considering the shaft power (Case A) and maximum with approximately 58% taking into account the shaft power and the kinetic exergy of the exhaust gaseous (Case B). The exergy consumption rate, the exergetic improvement potential rate and its percentage are indicated in Fig. 13. It shows that the maximum exergetic improvement potential was found to be 2117.04 kW with 33.7% – percentage improvement potential.
- The above-mentioned results clearly indicate that the combustion chamber, in which the combustion process occurred, has lower values of the exergy efficiency and higher values of the fuel exergy depletion, the productivity lack ratio, the relative exergy consumption and the exergetic improvement potential due to the combustion irreversibilities. Combustion of the fuel is a very complex phenomenon and it is highly thermodynamically irreversible process and limits the conversion of the fuel energy into the useful energy. Most of the combustion irreversibility is contributed to the internal heat transfer from burned fuel to the unburned fuel that is from products to reactants. Such heat transfer is inevitable in premix and diffusion flames where highly energetic molecules are free to exchange energy with un-reacted fuel and air mixture. For typical combustion systems, about 1/3rd of the fuel exergy becomes unavailable due to inherent the irreversibility in the combustor. Internal heat transfer, chemical reactions and mass transfer during combustion process generates entropy and reduces the potential of the products gases to do useful work [25].

For the maximum shaft power, the exergetic efficiency values of the T56 turboprop engine with a single-fixed shaft and the CT7-9C turboprop engine with free power turbine [13] are given in Table 12. When the results obtained from this study are compared with the results of CT7-9C turboprop engine;

- The exergetic efficiency of the CT7-9C's air compressor (AC) is higher than the T56 turboprop engine's due to the CT7-9C engine has five stages axial compressor and one stage centrifugal compressor that has a diffuser with the incorporation of quasi-rectangular passages that reduces losses and increases the compressor efficiency.
- The exergetic efficiency of the CT7-9C's combustion chamber (*CC*) is higher than the T56 turboprop engine's due to the CT7-9C engine's *CC* were made of the high temperature-resistant material and coated with thermal barrier coating. The CT7-9C engine is to be approximately 1547 K while the *CC* outlet temperature of the T56 turboprop engine is to be 1330 K.
- The exergetic efficiency values of the gas turbine (*GT*) component and the exhaust duct (*ED*) component of the T56 turboprop engine is higher than the components' of the CT7-9C engine. The higher stage number increases the pressure ratio and the efficiency of T56 engine's *GT*.
- The exergetic efficiency of the T56 turboprop engine is to be 23.8% while the exergetic efficiency of CT7-9C engine is to be 30%. The T56 engine was designed by the 1960s technologies. The CT7-9C engine has a higher efficiency due to that this engine produced in 1988 utilized a relatively new technology and an efficient combustion chamber.

4.3. Uncertainty analysis

The errors and uncertainties in the experimental can arise from the instrument selection, the instrument condition, the instrument calibration, the environment, the observation and the reading and the test planning. Uncertainty analysis is needed to prove the accuracy of experiments. An uncertainty analysis was performed using the method given in the literature [26,27]. The accuracy and the uncertainty of each measuring device given in Table 1 are checked yearly by the calibration laboratory. The accuracy and the uncertainty analysis of the test cell system are made during the calibration test run. The measurement data were taken from the calibration test run on September 25, 2012. The uncertainty values of some data, unchanged with the operation modes, are listed in Table 13. The uncertainty analysis of the measurement data and the calculated values that vary with the operation modes were performed in this study. The uncertainties of the measurement data (temperature, pressure, shaft power, thrust, etc.) were obtained from their repetitive measurements. The uncertainty values of the calculated data were determined from their functions. These are listed below:

- The uncertainty associated with the specific heat capacity was calculated as a function of the temperature.
- The uncertainties of the heat and work rates were estimated as a function of the mass flow, the specific heat capacity and the temperature.
- The uncertainties of exergy of the streams were accounted as a function of the mass flow, the specific heat capacity, the temperature and the pressure.

The nominal values (*NV*) and the percentage uncertainty (u_e) of the parameters changing with operation modes are given in Table 14. The nominal values (*NV*) and the percentage uncertainty (u_e) of the parameters changing with operation modes are given in Table 14. The uncertainties of the energy efficiency and the exergy efficiency values were calculated and added to Table 14. The uncertainties values of the measurement affect the energy efficiency that is to be ±0.135% at 75%-mode, ±0.129% at 100%-mode, ±0.130% at MIL-mode and ±0.133% at Takeoff-mode respectively. On the other hand, the uncertainties values of the measurement affect the exergy efficiency that is to be ±0.127% at 75%-mode, ±0.121% at 100%-mode and MIL-mode, and ±0.125% at Takeoff-mode. Considering the uncertainty values of the measurement and the calculated data, the deviations in the performance parameters of the engine may be assumed to be negligible.

5. Conclusions

This study presents the energy and exergy analysis of the T56 turboprop engine and its essential components at the different operation modes named 75%, 100%, MIL and Takeoff. The only one way of increasing the shaft power is to increase the fuel flow because the T56 turboprop engine is a fixed-single shaft constant-speed type turboprop engine. The produced shaft power and the residual thrust of the engine rise by increasing the fuel flow and the turbine inlet temperature according to the operation modes. The performance assessments were made for both the shaft power (Case A) and the shaft power plus the kinetic energy/exergy of exhaust gaseous (Case B). The energy and exergy analysis results of the whole engine indicate that the energy efficiency, the exergy efficiency and the improvement potential of the engine increase with taking into account the kinetic energy (exergy) of the exhaust gaseous to the engine products while the values of the energy losses rate, the exergy consumption rate, the fuel depletion ratio, the productivity lack ratio and the fuel-production ratio decrease.

The results of the component-based exergy analysis identify the combustion chamber between the components as having the most significant exergy consumption in the T56 turboprop engine, due to the irreversibilities associated with the combustion reaction and the heat transfer across the large temperature differences between burner gases and the working fluid. The exergy consumption rate of the combustion chamber increases from 4846.29 kW to 6234.13 kW while the exergy efficiency of the combustion chamber decreases from 66.83% to 66.04% by increasing the fuel flow and the turbine inlet temperature. The new design or modification of the combustion system should be investigated to increase its efficiency and the engine performance.

The methodology and the results of this study can be beneficial to those who deal with the analysis, determining the rooms for further improvement, and development of similar systems. For a future work, it is planned to perform an exergoeconomic analysis of the T56 turboprop engine to identify the cost flows of fuel, products and destructions to regulate the engine operation conditions and maintenances.

References

[1] Sehra AK, Whitlow Jr W. Propulsion and power for 21st century aviation. Prog Aerosp Sci 2004;40:199–235.
[2] Yılmaz I, Ilbas M, Tastan M, Tarhan C. Investigation of hydrogen usage in aviation industry. Energy Convers Manage 2012;63:63–9.
[3] Lee JJ. Can we accelerate the improvement of energy efficiency in aircraft systems? Energy Convers Manage 2010;51:189–96.
[4] Ozturk M, Ozek N, Yuksel YE. Gasification of various types of tertiary coals: a sustainability approach. Energy Convers Manage 2012;56:157–65.
[5] Rosen MA. Assessing energy technologies and environmental impacts with the principles of thermodynamics. Appl Energy 2002;72(1):427–41.
[6] Rosen MA, Dincer I. Exergoeconomic analysis of power plants operating on various fuels. Appl Therm Eng 2003;23:643–58.
[7] Etele J, Rosen MA. Sensitivity of exergy efficiencies of aerospace engines to reference environment selection. Exergy Int J 2001;1(2):91–9.
[8] Turgut ET, Karakoc TH, Hepbasli A. Exergetic analysis of an aircraft turbofan engine. Int J Energy Res 2007;31(14):1383–97.
[9] Turan O. Effect of reference altitudes for a turbofan engine with the aid of specific-exergy based method. Int J Exergy 2012;11(2):252–70.
[10] Ahmadi P, Dincer I. Thermodynamic analysis and thermoeconomic optimization of a dual pressure combined cycle power plant with a supplementary firing unit. Energy Convers Manage 2011;52:2296–308.
[11] Balli O, Aras H, Aras N, Hepbasli A. Exergetic and exergoeconomic analysis of an Aircraft Jet Engine (AJE). Int J Exergy 2008;5(5/6):567–81.
[12] Turgut ET, Karakoc TH, Hepbasli A. Exergoeconomic analysis of an aircraft turbofan engine. Int J Exergy 2009;6(3):277–94.
[13] Aydin H, Turan O, Midilli A, Karakoc TH. Exergetic and exergo-economic analysis of a turboprop engine: a case study for CT7-9C. Int J Exergy 2012;11(1):69–82.
[14] Meyer L, Tsatsaronis G, Buchgeister J, Schebek L. Exergoenvironmental analysis for evaluation of the environmental impact of energy conversion systems. Energy 2009;34:75–89.
[15] Altuntas O, Karakoc TH, Hepbasli A. Exergoenvironmental analysis of piston-prop aircrafts. Int J Exergy 2012;10(3):290–8.
[16] Bejan A, Siems D. The need for exergy analysis and thermodynamic optimization in aircraft development. Exergy Int J 2001;1(1):14–24.
[17] Tona C, Raviolo PA, Pellegrini LF, Oliveria Jr S. Exergy and thermodynamic analysis of a turbofan engine during a typical commercial flight. Energy 2010;35(2):952–9.
[18] Riggings D. The thermodynamic continuum of jet engine performance: the principle of lost work due to irreversibility in Aerospace systems. Int J Thermodyn 2003;6(3):107–20.
[19] Dincer I, Cengel YA. Energy, entropy and exergy concepts and their roles in thermal engineering. Entropy 2001;3:116–49.
[20] Balli O, Aras H, Hepbasli A. Thermodynamic and thermoeconomic analyses of a trigeneration (TRIGEN) system with a gas–diesel engine: Part I-Metdodology. Energy Convers Manage 2010;51:2252–9.
[21] Mansouri MT, Ahmadi P, Kaviri AG, Jaafar MNM. Exergetic and economic evaluation of the effect of HRSG configurations on the performance of combined cycle power plants. Energy Convers Manage 2012;58:47–58.
[22] Silveira JL, Beyene A, Leal EM, Santana JA, Okada D. Thermoeconomic analysis of a cogeneration system of a university campus. Appl Therm Eng 2002;22:1471–83.
[23] Rakopoulos CD, Giakoumis EG. Second-law analyses applied to internal combustion engines operations. Prog Energy Combust Sci 2006;32:2–47.
[24] Aydın H, Turan O, Karakoc TH, Midilli A. Component-based exergetic measures of an experimental turboprop/turboshaft engine for propeller aircrafts and helicopters. Int J Exergy 2012;11(3):322–48.
[25] Karimi MN, Kamboj SK. Exergy destruction and chemical irreversibilities during combustion in spark-ignition engine using oxygenated and hydrocarbon fuels. Int J Mech Ind Eng (IJMIE) 2012;2(3):7–11.
[26] Hepbasli A, Akdemir O. Energy and exergy analysis of a ground source (geothermal) heat pump system. Energy Convers Manage 2004;45:737–53.
[27] Dogru M, Midilli A, Howarth CR. Gasification of sewage sludge using a throated downdraft gasifier and uncertainty analysis. Fuel Process Technol 2002;75:55–82.